An Improved GPS-Based Precise Point Positioning Model

Mohamed Elsobeiey and Ahmed El-Rabbany, Canada

Key words: GPS, Precise Point Positioning, second order ionospheric delay

SUMMARY

In this paper we introduce an improved Precise Point Positioning (PPP) model, which rigorously accounts for all GPS errors and biases including the second-order ionospheric delay, which is the most significant among the higher-order ionospheric delay terms. We use between-satellite single-difference (BSSD), which cancels out the receiver hardware delay, receiver clock error, and the non-zero initial phase of the receiver's oscillator. Tropospheric delay is accounted for using the NOAA-based numerical weather prediction (NWP) tropospheric signal delay model (NOAATrop). The NOAATrop model was extensively tested and found superior to standard tropospheric models such as the Saastamoinen and Hopfield models. All remaining errors, including carrier-phase windup, relativity, sagnac, Earth tides, and ocean loading can be accounted for with sufficient accuracy using existing models.

It is shown that the PPP solution convergence time is improved by up to 30% when using our BSSD-based model in comparison with traditional undifferenced PPP model. This is considered significant and can lead to the development of high-accuracy real-time PPP. In addition, the RMS of the estimated parameters is improved up to 40%.

An Improved GPS-Based Precise Point Positioning Model

Mohamed Elsobeiey and Ahmed El-Rabbany, Canada

1. INTRODUCTION

Typically, differential mode is used for GPS applications requiring high accuracy. A major disadvantage of GPS differential positioning, however, is its dependency on the measurements or corrections from a reference station; i.e., two or more GPS receivers are required to be available. Since the termination of selective availability in 2000, it became possible to achieve autonomous positioning accuracy comparable to that of differential mode. Unlike the differential mode where most GPS errors and biases are essentially cancelled, all errors and biases must be rigorously modeled in PPP. Typically, undifferenced ionosphere-free linear combination of code and carrier-phase observations is used to remove the first-order ionospheric effect. This linear combination, however, leaves a residual ionospheric delay of up to a few centimeters representing higher-order ionospheric terms (Hoque and Jakowski, 2007, 2008). Satellite orbit and satellite clock errors can be accounted for using precise orbit and clock products from, for example, International GNSS Service (IGS). Receiver clock error can be estimated as one of the unknown parameters. The effects of ocean loading, Earth tide, carrier-phase windup, sagnac, relativity, and satellite and receiver antenna phase-center variations can sufficiently be modeled or calibrated. Tropospheric delay can be accounted for using empirical models (e.g. Saastamoinen or Hopfield models) or by using tropospheric corrections derived from regional GPS networks such as the NOAA tropospheric corrections (NOAATrop). The NOAATrop model incorporates GPS observations into numerical weather prediction (NWP) models (Gutman et al., 2003).

This paper uses between-satellite single-difference model to cancel out all receiver-related errors such as receiver clock error, receiver hardware delay, and receiver initial phase bias. A complete model for second-order ionospheric delay is also included. Tropospheric delay is accounted for using the NOAATrop model. It is shown that accounting for the second-order ionospheric delay and using BSSD model improves the PPP convergence time by about 30% and the RMS of the estimated parameters is improved up to 40%.

2. GPS OBSERVATION EQUATIONS

The mathematical models of undifferenced GPS pseudorange and carrier-phase measurements can found in Hofmann-Wellenhof et. al. (2008) and Leick (2004). Considering the second-order ionospheric delay (Bassiri and Hajj, 2003) and satellite and receiver differential code bias (Schaer and Steigenberger, 2006; Dach et al., 2007), the mathematical models of undifferenced GPS pseudorange and carrier-phase measurements can be written as:

$$P_1 = \rho + c(dt^r - dt^s) + T + \frac{q}{f_1^2} + \frac{s}{f_1^3} + c(d_{P1}^r - d_{P1}^s) + \varepsilon_{P1} \quad (1)$$

$$P_2 = \rho + c(dt^r - dt^s) + T + \frac{q}{f_2^2} + \frac{s}{f_2^3} + c(d_{P2}^r - d_{P2}^s) + \varepsilon_{P2} \quad (2)$$

$$\Phi_1 = \rho + c(dt^r - dt^s) + T - \frac{q}{f_1^2} - \frac{s}{2f_1^3} + c(\delta_{\Phi1}^r - \delta_{\Phi1}^s) + \lambda_1\left[N_1 + \phi_{\Phi1}^r(t_0) - \phi_{\Phi1}^s(t_0)\right] + \varepsilon_{\Phi1} \quad (3)$$

$$\Phi_2 = \rho + c(dt^r - dt^s) + T - \frac{q}{f_2^2} - \frac{s}{2f_2^3} + c(\delta_{\Phi2}^r - \delta_{\Phi2}^s) + \lambda_2\left[N_2 + \phi_{\Phi2}^r(t_0) - \phi_{\Phi2}^s(t_0)\right] + \varepsilon_{\Phi2} \quad (4)$$

where,

P_1, P_2	pseudorange measurements on L1 and L2, respectively
Φ_1, Φ_2	carrier-phase measurements on L1 and L2, respectively, scaled to distance (m)
ρ	the true geometric range from receiver antenna phase-centre at reception time to satellite antenna phase-centre at transmission time (m)
f_1, f_2	L1 and L2 frequencies, respectively, ($L_1 : f_1 = 1.57542\ GHz$; $L_2 : f_2 = 1.22760\ GHz$)
dt^r, dt^s	receiver and satellite clock errors, respectively
T	topospheric delay error
λ_1, λ_2	the wavelengths for L1 and L2 carrier frequencies, respectively
N_1, N_2	integer ambiguity parameters for L1 and L2, respectively
δ_*^r, δ_*^s	frequency-dependent carrier-phase hardware delay for receiver and satellite, respectively
d_*^r, d_*^s	code hardware delay for receiver and satellite, respectively
c	the speed of light in vacuum
$\phi_*^r(t_0), \phi_*^s(t_0)$	receiver and satellite non-zero initial phase bias, respectively
q	the total electron content integrated along the line of sight
s	the second-order ionospheric effect
$\varepsilon_{P1}, \varepsilon_{P2}, \varepsilon_{\Phi1}, \varepsilon_{\Phi2}$	the unmodelled error sources including orbital error, multipath effect,

and others

Typically the first-order ionosphere-free linear combination is used by the IGS and its analysis centers to estimate the satellite clock correction. The code pseudorange represents the datum for the estimated satellite clock corrections and the code hardware delays are neglected during the estimation process. Define $\xi_1 = \frac{f_1^{\,2}}{f_1^{\,2} - f_2^{\,2}}$ and $\xi_2 = \frac{f_2^{\,2}}{f_1^{\,2} - f_2^{\,2}}$, the well-known ionosphere-free linear combination can be formed to eliminate the first-order ionospheric delay as,

$P_3 = \xi_1 P_1 - \xi_2 P_2,\ \ \Phi_3 = \xi_1 \Phi_1 - \xi_2 \Phi_2$

$$P_3 = \rho + c(dt^r - dt^s) + T + \frac{s}{f_1 f_2 (f_1 + f_2)} + b_{P3}^r - b_{P3}^s + \varepsilon_{P3} \tag{5}$$

$$\Phi_3 = \rho + c(dt^r - dt^s) + T - \frac{s}{2 f_1 f_2 (f_1 + f_2)} + b_{\Phi 3}^r - b_{\Phi 3}^s + \lambda_3 N_3 + \varepsilon_{\Phi 3} \tag{6}$$

where;

$$s = 7527 * c * B_0 * \cos(\theta) * STEC \tag{7}$$

$$STEC = \left[(P_2 - P_1) + c(DCB_{P1-P2}^r + DCB_{P1-P2}^S) \right] \left(\frac{f_2^{\,2}}{f_1^{\,2} - f_2^{\,2}} \right) \left(\frac{f_1^{\,2}}{40.3} \right) \tag{8}$$

$b_{P3}^r = c\left(\xi_1 d_{P1}^r - \xi_2 d_{P2}^r\right)$

$b_{P3}^s = c\left(\xi_1 d_{P1}^s - \xi_2 d_{P2}^s\right)$

$b_{\Phi 3}^r = \left[c\left(\xi_1 \delta_{\Phi 1}^r - \xi_2 \delta_{\Phi 2}^r\right) + \left(\xi_1 \lambda_1 \phi_{\Phi 1}^r(t_0) - \xi_2 \lambda_2 \phi_{\Phi 2}^r(t_0)\right) \right]$

$b_{\Phi 3}^s = \left[c\left(\xi_1 \delta_{\Phi 1}^s - \xi_2 \delta_{\Phi 2}^s\right) + \left(\xi_1 \lambda_1 \phi_{\Phi 1}^s(t_0) - \xi_2 \lambda_2 \phi_{\Phi 2}^s(t_0)\right) \right]$

$\lambda_3 = \frac{c}{\left(f_1^{\,2} - f_2^{\,2}\right)}, N_3 = \left(f_1 N_1 - f_2 N_2\right)$

P_3, Φ_3	the first-order ionosphere-free code and carrier-phase combinations, respectively
$\varepsilon_{P3}, \varepsilon_{\Phi 3}$	the first-order ionosphere-free combination of $\varepsilon_{P1}, \varepsilon_{P2}$ and $\varepsilon_{\Phi 1}, \varepsilon_{\Phi 2}$, respectively
B_0	the magnetic field at the ionospheric pierce point (IPP)
θ	the angle between the magnetic field and the propagation direction
STEC	slant total electron content along the signal propagation direction
$DCB_{P1-P2}^r, DCB_{P1-P2}^S$	P1-P2 receiver and satellite differential code bias, respectively

3. CORRECTION FOR THE SECOND-ORDER IONOSPHERIC DELAY

The second-order ionospheric delay results from the interaction of the ionosphere and the magnetic field of the Earth (Hoque and Jakowski, 2008). As seen in Equations 7, the second-order ionospheric delay depends on the STEC and the magnetic field parameters. The STEC may be obtained from agencies such as the IGS and NOAA. IGS produces global ionospheric maps (GIMs) in the ionospheric exchange (IONEX) format (Schaer et al., 1998). Alternatively, STEC can be estimated by forming the geometry-free linear combination of GPS pseudorange observables and applying the corresponding differential code biases (Equation 8). Magnetic field parameter, on the other hand, can be obtained from the international geomagnetic reference field (IGRF). It should be noted that second-order ionospheric delay should be considered when estimating the GPS satellite orbit and clock corrections. More details about the impact of second-order ionospheric delay on GPS satellite orbit and clock corrections can be found in Elsobeiey and El-Rabbany, 2011.

4. BETWEEN-SATELLITE SINGLE-DIFFERENCE MODEL

Between-satellite single difference cancels out the receiver-originating errors and biases, including receiver clock error, receiver hardware delay, and non-zero initial phase of the receiver's oscillator. However, differencing observations between satellites causes mathematical correlations among the observations, which must be considered when forming the covariance matrix of the observation. Starting from Equations (5) and (6), we can get the ionosphere-free BSSD for satellites *k* and *l* as:

$$P_3^{kl} = \rho^k - \rho^l + c(dt_{P3}^l - dt_{P3}^k) + T^k - T^l \tag{9}$$

$$L_3^{kl} = \rho^k - \rho^l + c(dt_{P3}^l - dt_{P3}^k) + T^k - T^l + \lambda_3\left(N_3''^k - N_3''^l\right) \tag{10}$$

where $N_3'' = (b_{P3}^s - b_{\Phi 3}^s)/\lambda_3 + N_3$. As can be noted, the receiver hardware delay and non-zero initial phase are cancelled out.

To test the developed models, GPS data from 5 randomly-selected IGS stations were processed (Figure 1). The data used were the ionosphere-free (with both first- and second-order corrections included) linear combination of pseudorange and carrier-phase measurements. The precise orbit and clock corrections after accounting for the second-order ionospheric delay are applied (see Elsobeiey and El-Rabbany, 2011). NOAATrop model is used to account for the tropospheric correction (Gutman et al., 2003; Ibrahim and El-Rabbany 2008) along with Vienna mapping function 1 (Boehm et al. 2006). The processing is carried out in two steps; first by using the one way processing model (Equations 5 and 6), second by using the BSSD model (Equations 9 and 10). The results show that improvements are attained in all three components of the station coordinates. Figures 2 through 7 show the 3D solutions obtained from the two solutions for stations ALGO and ALBH, as examples. As can be seen,

the amplitude variation of the estimated coordinates during the first 20 minutes is reduced when using the BSSD model and considering the second-order ionospheric delay and apply NOAATrop corrections. In addition, the convergence time for the estimated parameters is reduced by about 30% in average. The final PPP solution shows an average improvement of 40% in the RMS of the estimated coordinates. Table 1 summarizes the RMS of the final solution of 1 hour of data of all stations. It should be pointed out that the correction for the second-order ionospheric delay improves the convergence time of the horizontal components (latitude and longitude). However, the improvement in the height component is attributed to the combined effect of second-order ionospheric corrections and NOAATrop corrections. BSSD, on the other hand, improves the convergence time of the station coordinates (latitude, longitude, and height) as depicted in Figures 2 through 7).

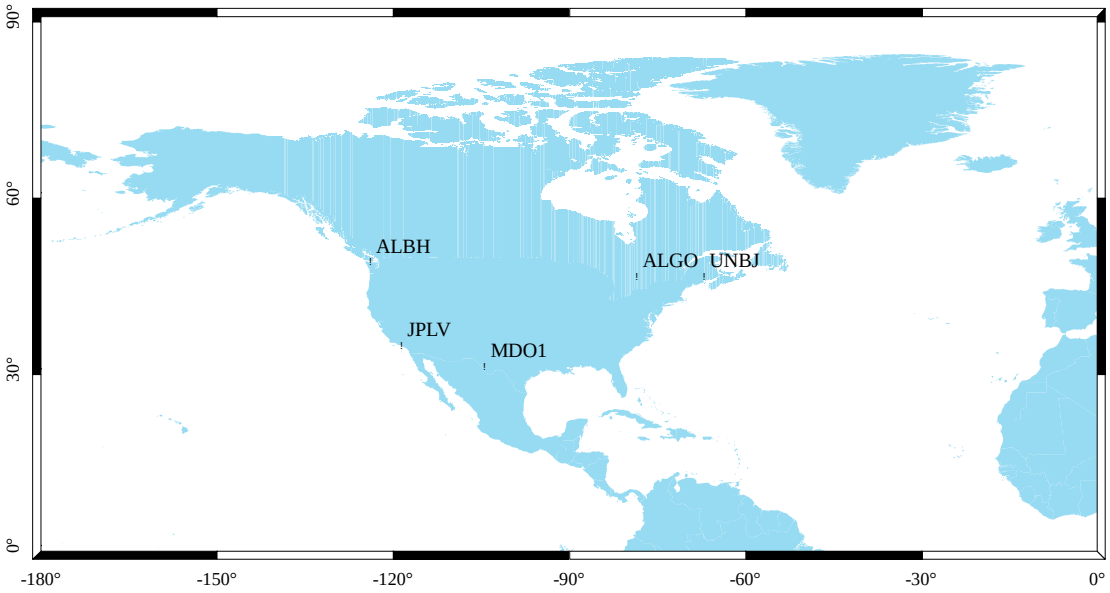

Figure 1. IGS Stations Used in Verification of the Developed Models

Table 1: RMS of the Final Solution (1 hour of data) of the Tested IGS Stations

Processing Mode	Un-Differenced + 1st Order IONO RMS (mm)				BSSD + 1st + 2nd Order IONO + NOAATrop RMS (mm)			
Station	Lat.	Lon.	Ht.	3D	Lat.	Lon.	Ht.	3D
ALBH	2.9	7.1	8.0	11.1	1.8	4.2	5.2	6.9
ALGO	7.1	14.5	13.8	21.2	2.8	5.9	5.6	8.6
MDO1	7.3	6.5	9.1	13.5	5.3	4.5	7.0	9.8
JPLV	4.6	8.7	15.9	18.7	3.1	5.9	8.7	11.0
UNBJ	5.5	4.8	8.1	10.9	3.2	3.5	4.9	6.8

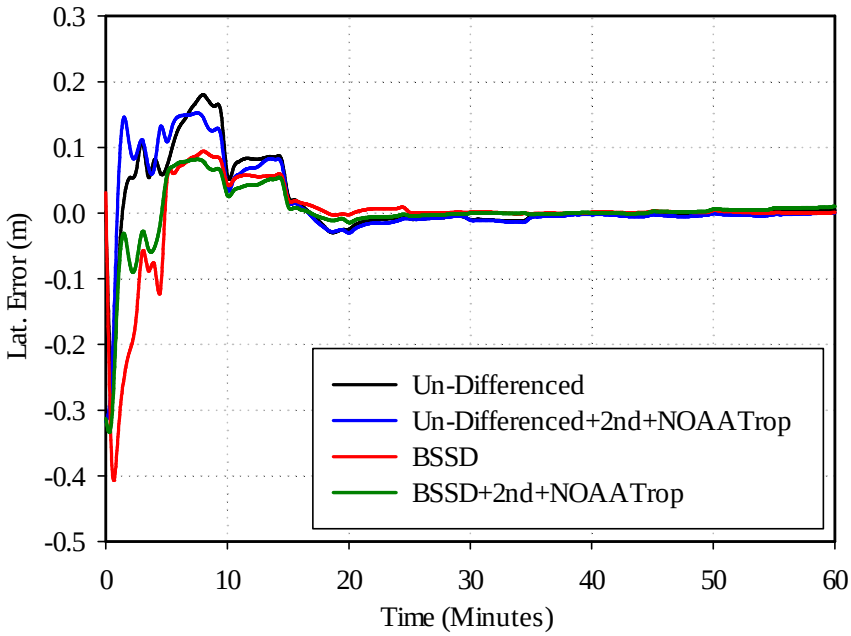

Figure 2. Latitude Improvement Using BSSD Model, Accounting for Second-Order Ionospheric Delay, and NOAATrop at ALGO IGS Station, DOY125, 2010

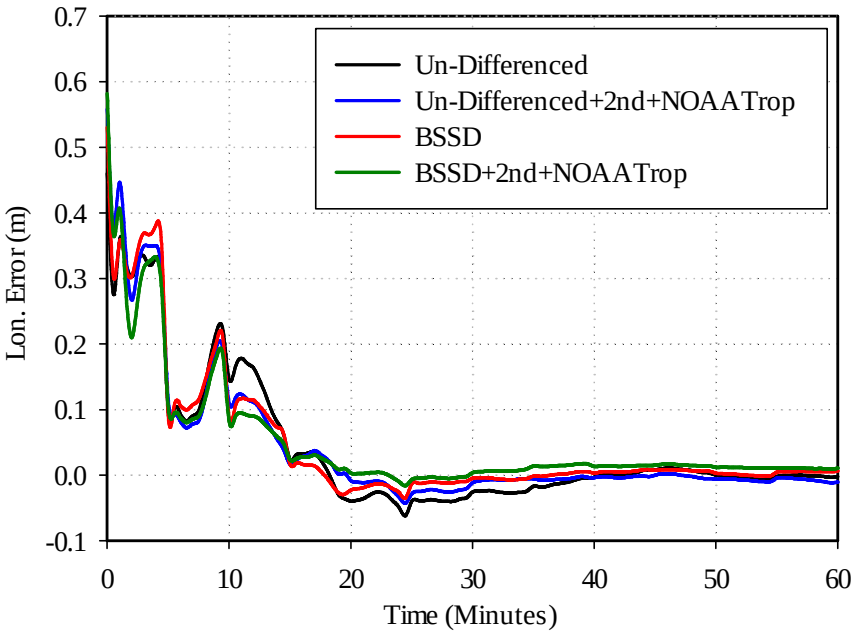

Figure 3. Longitude Improvement Using BSSD Model, Accounting for Second-Order Ionospheric Delay, and NOAATrop at ALGO IGS Station, DOY125, 2010

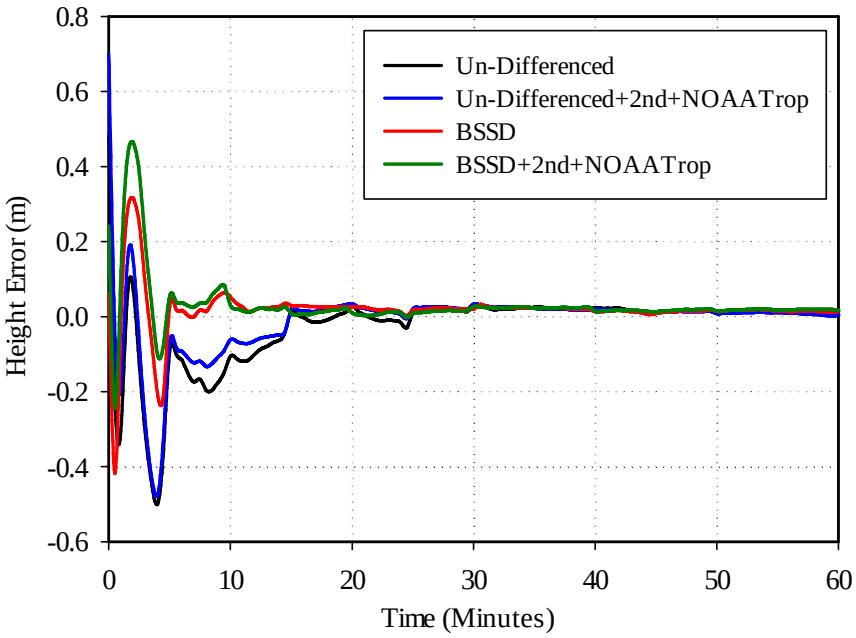

Figure 4. Ellipsoidal Height Improvement Using BSSD Model, Accounting for Second-Order Ionospheric Delay, and NOAATrop at ALGO IGS Station, DOY125, 2010

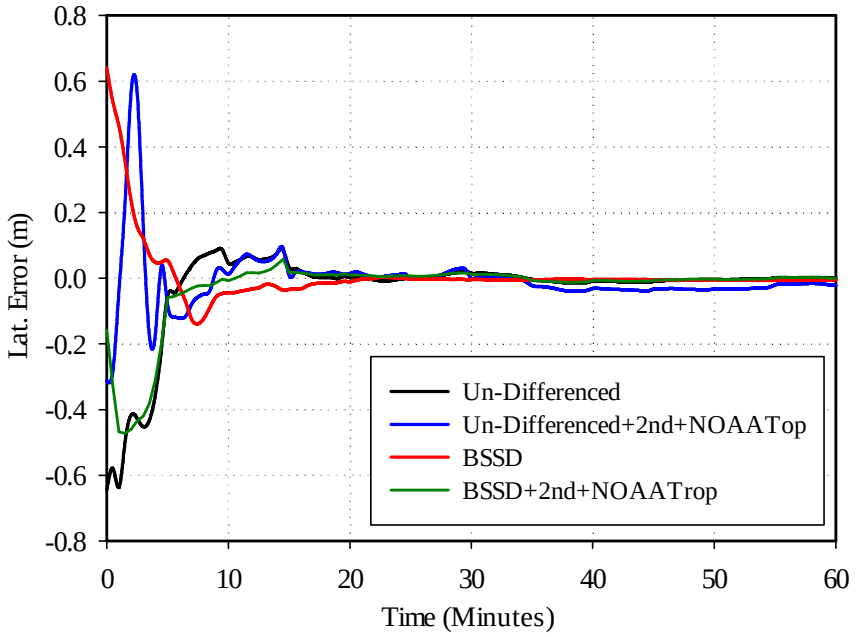

Figure 5. Latitude Improvement Using BSSD Model, Accounting for Second-Order Ionospheric Delay, and NOAATrop at ALBH IGS Station, DOY125, 2010

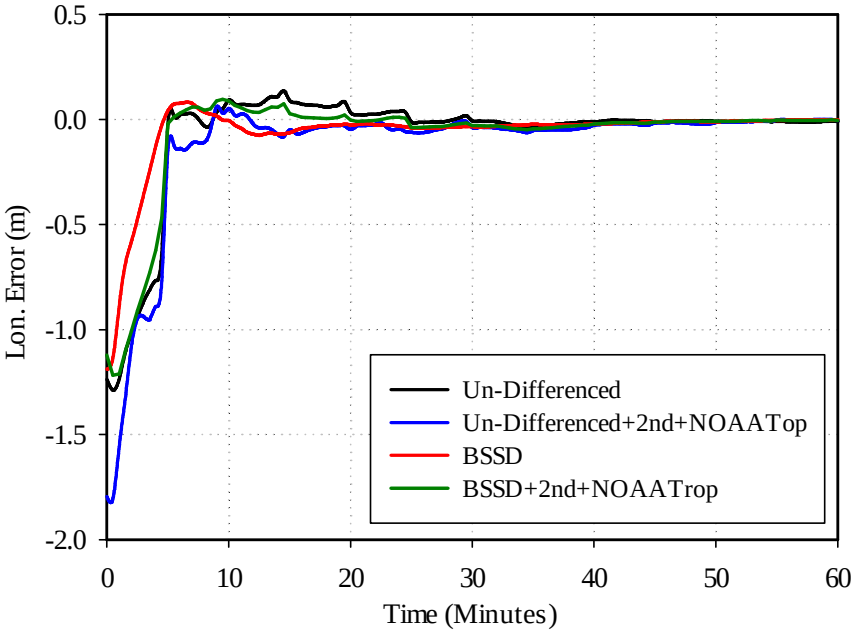

Figure 6. Longitude Improvement Using BSSD Model, Accounting for Second-Order Ionospheric Delay, and NOAATrop at ALBH IGS Station, DOY125, 2010

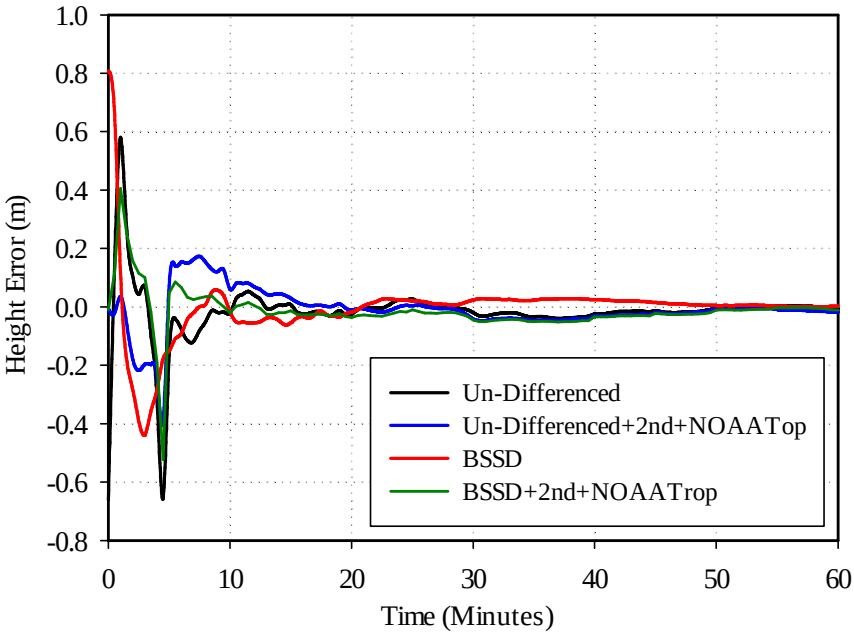

Figure 7. Ellipsoidal Height Improvement Using BSSD Model, Accounting for Second-Order Ionospheric Delay, and NOAATrop at ALBH IGS Station, DOY125, 2010

5. CONCLUSIONS

It has been shown that ionosphere-free between-satellite single difference model significantly improves the PPP convergence time and solution. BSSD model cancels out receiver clock error and also the receiver hardware delay and initial phase bias, which not easy to model and usually neglected in the one way PPP model. It is shown also that BSSD model is superior to the standard un-differenced PPP model as it improves the final PPP coordinate solution RMS up to 40% and improves the convergence time of the estimated parameters by about 30%.

6. ACKNOWLEDGMENTS

This research was supported in part by the GEOIDE Network of Centres of Excellence (Canada) and by the Natural Sciences and Engineering Research Council (NSERC) of Canada. The data sets used in this research were obtained from the IGS website http://igscb.jpl.nasa.gov/.

7. REFERENCES

Bassiri, S. and G. Hajj, 1993. High-order ionospheric effects on the global positioning system observables and means of modeling them, Manuscr. Geod., 18, pp 280– 289

Boehm, J., B. Werl and H. Schuh, 2006. Troposphere mapping functions for GPS and very long baseline interferometry from European Centre for Medium-Range Weather Forecasts operational analysis data. J Geophys Res 111:B02406. doi:10.1029/2005JB003629

Dach, R., U. Hugentobler, P. Fridez, and M. Meindl, 2007. Bernese GPS Software Version 5.0. Astronomical Institute, University of Berne, Switzerland.

Elsobeiey, M. and A. El-Rabbany (2011). Impact of Second-Order Ionospheric Delay on Precise Point Positioning. Journal of Applied Geodesy. DOI: 10.1515/JAG.2011.004.

Gutman, S., T. Fuller-Rowell, D. Robinson, 2003. Using NOAA Atmospheric Models to Improve Ionospheric and Tropospheric Corrections. U.S. Coast Guard DGPS Symposium, Portsmouth, VA, 19 June.

Hofmann-Wellenhof, B., H. Lichtenegger, and E. Walse, 2008. GNSS Global Navigation Satellite Systems; GPS, Glonass, Galileo & more. Springer Wien, New York

Hoque, M. and N. Jakowski, 2007, Higher order ionospheric effects in precise GNSS positioning. Journal of Geodesy Vol. 81, pp 259-268.

Hoque, M. and N. Jakowski, 2008. Mitigation of higher order ionospheric effects on GNSS users in Europe. GPS solutions Vol. 12, No. 2, pp 87-97.

Houghton, J. T., M. J. Rycroft, and A. J. Dessler, 1998. Physics of the space environment. Cambridge University Press, 1998.

Ibrahim, H. E. and A. El-Rabbany, 2008. Regional Stochastic Models for NOAA-Based Residual Tropospheric Delays. The Journal of Navigation 61: 209-219.

Leick, A., 2004. GPS Satellite Surveying. 3rd edition, John Wiley and Sons.

Schaer, S., G. Beutler, and M. Rothacher, 1998. Mapping And Predicting The Ionosphere. Proceeded in the IGS Analysis Centre Workshop, Darmstadt, Germany, February 9–11

Schaer, S., S. Steigenberger, 2006. Determination and Use of GPS Differential Code Bias Values. IGS Analysis Centre Workshop, Darmstadt, Germany.